Joint EUROGRAPHICS - IEEE TCVG Symposium on Visualization (2004)
O. Deussen, C. Hansen, D.A. Keim, D. Saupe (Editors)

# Accuracy Evaluation of Different Centerline Approximations of Blood Vessels

A. La Cruz

Institute of Computer Graphics and Algorithms, Vienna University of Technology

**Abstract**

*Accurate determination of the vessel axis is a prerequisite for automated visualization and quantification of artery diseases. This paper presents an evaluation of different methods for approximating the centerline of the vessel in a phantom simulating the peripheral arteries. Six algorithms were used to determine the centerline of a synthetic peripheral arterial vessel. They are based on: ray casting using thresholds and maximum gradient-like stop criterion, pixel motion estimation between successive images called block matching, center of gravity and shape based segmentation. The Randomized Hough Transform and ellipse fitting have been used as shape based segmentation techniques. Since in the synthetic data set the centerline is known, an estimation of the error can be calculated in order to determine the accuracy achieved by a given method.*

Categories and Subject Descriptors (according to ACM CCS): I.3.3 [Blood Vessel]: Centerline detection, Vessel segmentation, Medical Visualization

## 1. Introduction

Epidemiological and clinical studies have shown that peripheral arterial occlusive disease (PAOD) increases the risk of cardiovascular and cerebrovascular events and mortality [PGJ03]. CT-angiography (CTA) is a routinely applicable non-invasive vascular imaging technique for many vascular territories such as the peripheral (lower extremity) arteries. Accurate identification of the vessel centerline in CTA data sets is highly desirable, because of its crucial role in vessel visualization (e.g., through curved planar reformations - CPR [KPF*01]) and automated vessel analysis and quantification.

The vessel centerline is widely used for 3D reconstruction and modelling of vessel structures. It has been used as a basis for several vessel segmentation techniques [KQ00], and as starting point for a geometric model definition of vascular structures [BFC03]. The skeletonization of a vascular structure is a method widely used for centerline detection [Pui98]. Several methods based on the skeletonization use thresholds and object connectivity [NKSK93], distance field calculation [Pui98], mathematical morphology based on dilation, erosion, opening and closing operators [TKN*95]. These approaches have been applied on different image modalities (e.g., MRI, CTA) and vascular structures. Many of them have been applied on a specific part of the vessel structure, for example, cerebrovascular structures [Pui98], coronary arteries from biplane angiograms [CRC92] or aorta [WNV00]. These techniques and methods have not been applied to the centerline detection of peripheral vessels, where the level of intensity decreases from top to bottom, from aorta to pedal (tibial and fibular arteries). For peripheral arteries, an accurate detection of the centerline is very difficult, specifically where the diameter can be between only two to four voxels. The partial volume effect also makes correct identification of small vessels (e.g. tibial and fibular arteries) difficult.

This work presents the results of an accuracy evaluation of six techniques for approximating the vessel centerline in peripheral arteries. This paper has the following structure. Section 2 describes each method which has been evaluated. Section 3 presents the evaluation and the results. Finally, section 4 presents the conclusions and future work.

## 2. Centerline Approximation Methods

Starting from an initial path of the vessel, six different techniques to approximate the vessel centerline have been used in order to evaluate accuracy and quality. This initial path is

estimated using the vessel tracking technique developed by Kanitsar et al. [KPF*01]. This technique consists of finding the path with the minimum cost. The cost is defined by a cost function which depends on a value associated to the density for vessels *vs* other tissues, Laplacian filter and the gradient magnitude between two adjacent voxels along the path.

The path generated by vessel tracking is with high probability inside the vessel structure and is taken as basis to apply the different centerline approximation methods. Along this path, a perpendicular cross-section is estimated for each point. Each center approximation technique presented in the following sections is applied to each perpendicular cross-section (on a 2D plane). The vessel centerline is defined as a 3D curve smoothed using B-splines.

### 2.1. Ray Casting

Ray casting methods trace several rays from one point inside the object to the outside. The idea is to trace several rays $\vec{r}$ (see Figure 1) from one initial point inside the object until a boundary is detected. Wink et al. [WNV00] and Kanitsar et al. [KPF*01] use this technique to approximate the vessel centerline.

Wink et al. [WNV00] use gradient information to detect the border of the vessel. First, they calculate the gradient via convolution of the original image with a normalized Gaussian derivative, in order to reduce noise and other irregularities in the image. Then, they define the border as the position where the gradient magnitude in the direction of the ray reaches a first maximum above some threshold. The threshold has to be significantly higher than the typical noise level in the data set. This threshold depends on the image quality (e.g., contrast, noise and resolution), and is therefore modality-dependent. On the other hand, Kanitsar et al. [KPF*01] apply ray casting technique based on a valid density interval for vessels, and stop a cast ray when a density value along the ray is outside this interval. This valid interval for a vessel was defined empirically between $t_{lower}$ and $t_{upper}$.

Two techniques based on ray casting were implemented. One is denoted as ray casting with thresholds (RCT) and the other as ray casting with maximum gradient (RCMG). The RCT is the same ray casting technique used by Kanitsar [KPF*01]. RCMG uses the maximum gradient along the ray as stopping criterion. Furthermore, the RCMG method uses also the lower threshold value $t_{lower}$ to validate that tissues with lower density than the density for vessels are not considered. After several border points are estimated, the true center is calculated by:

$$[x_c, y_c] = \left[ \frac{\sum_{i=1}^{n} x_i (d_{i-1} + d_{(i)mod(n)})}{2\sum_{i=1}^{n} d_i}, \frac{\sum_{i=1}^{n} y_i (d_{i-1} + d_{(i)mod(n)})}{2\sum_{i=1}^{n} d_i} \right] \quad (1)$$

Here, $x_c$ and $y_c$ are the coordinates of the center calculated, $n$ is the number of border points detected, $x_i$ and $y_i$ are the coordinates of the *i-th* border point, and $d_i$ is the distance between two adjacent border points $i$ and $i+1$. The function *mod* is used due the circular connection between successive border points.

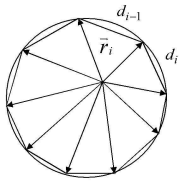


**Figure 1:** *Example of the ray casting method*

### 2.2. Block Matching

Block Matching (BM) technique is used for motion estimation between successive frames in video compression. More details are described in [DKF95]. Assume that two 2D images are related by a simple shift determined by $x_d$ and $y_d$. These values are estimated by minimizing the magnitude of the difference between shifted states of the two images as:

$$(x_d, y_d) = min_{x'_d, y'_d} \sum_{i,j} \left[ f_{2D}(i + x'_d, j + y'_d, 1) - f_{2D}(i, j, 0) \right]^2, \quad (2)$$

where $x'_d$ and $y'_d$ are the displacements of pixels in image space.

This method is applied incrementally for pairs of successive cross-sections of the initial vessel path. It looks for the best matching between two vessel cross-sections by applying a shift on the original cross-sections. The consecutive cross-section is shifted to several new positions and matched with the previous cross-section. The best match result is selected as center of the vessel.

### 2.3. Center Of Gravity

The weighted center of gravity (CoG) has been used widely for estimation of object centers in gray level images with sub-pixel precision [vAEPR02]. The center of gravity can be defined as the equilibrium point where the entire weight of the object is concentrated. For a $2D$ gray level image the center of gravity is defined in [vAEPR02] as:

$$[x_c, y_c] = \left( \frac{\sum_{x,y \in \Omega} x\, w(x,y)}{\sum_{x,y \in \Omega} w(x,y)}, \frac{\sum_{x,y \in \Omega} y\, w(x,y)}{\sum_{x,y \in \Omega} w(x,y)} \right), \quad (3)$$

where $\Omega$ defines the area containing pixels that belong to the vessel. $w(x,y)$ is the weight for each coordinate in the $\Omega$ space, and can be defined as:

$$w(x,y) = f_{2D}(x,y) - m \quad (4)$$

and,

$$m = min_{x,y \in \Omega}(f_{2D}(x,y)) \quad (5)$$

The function $f_{2D}(x,y)$ corresponds to the density value of a pixel $(x,y)$ in the perpendicular 2D cross-section.

The threshold values $t_{lower}$ and $t_{upper}$ defined for RCT technique, were used also in this method to determine those points which belong with high probability to the blood vessel.

### 2.4. Ellipse Fitting

Blood vessels have a tubular structure, which can be defined by a set of elliptical shapes along its axis. Therefore, an approximation of the centerline of the vessel can be estimated as the center of an elliptical shape along its axis. This technique is denoted as EF. Starting from the initial path obtained via vessel tracking, the Canny edge detector [Can86] is applied in order to get a set of points around the vessel boundary. Then, these points are approximated with an ellipse using the Lagrange multiplier technique. The problem can be described as:

Given:

- A set of 2D Points $P = \{\mathbf{x}_i\}_{i=1}^{n}$, where $\mathbf{x}_i = (x_i, y_i)$
- A curve $C(\mathbf{a})$ characterized by the vector $\mathbf{a}$. Where $C(\mathbf{a}) = \{\mathbf{x} | F(\mathbf{a}, \mathbf{x}) = 0\}$, in our case $F(\mathbf{a}, \mathbf{x})$ is the representation of general conic curves which is given by:

$$\begin{aligned} F(\mathbf{a}, \mathbf{x}_i) &= ax_i^2 + bx_iy_i + cy_i^2 + dx_i + ey_i + f \\ &= \left[x_i^2, x_iy_i, y_i^2, x_i, y_i, 1\right][a, b, c, d, e, f]^T, \end{aligned} \quad (6)$$

  with $\mathbf{a} = [a, b, c, d, e, f]$ and $\mathbf{x}_i = [x_i^2, x_iy_i, y_i^2, x_i, y_i, 1]$
- A distance metric $\delta(C(\mathbf{a}), \mathbf{x})$ as a measure of the distance from a point $\mathbf{x}$ to the curve $C(\mathbf{a})$. Defined by $F(\mathbf{a}, \mathbf{x}_i)^2$.

The problem consists of minimizing the sum of squared algebraic distances $\sum_{i=1}^{n} F(\mathbf{a}, \mathbf{x}_i)^2$ with the constraint that for an ellipse $4ac - b^2 = 1$. After this optimization problem is solved [FF95], the ellipse center and axis can be extracted using equation (6).

### 2.5. Randomized Hough Transform

The randomized Hough Transform (RHT) technique introduced by Xu et al. [XOK90] consists of randomly selecting a subset of points from an image and fitting a parameterized curve to them.

First, the Canny edge detector is applied [Can86] in order to get a binary edge image. Then, parametric ellipses are extracted using the technique defined by MacLaughlin [Mac98]. He describes a method to accelerate the ellipse detection in an image using the RHT. This technique consists of randomly selecting three points ($P_1$, $P_2$, $P_3$) from the binary edge image, and defining the ellipse that passes through these points (see Figure 2). For each point $P_i$ the tangent to the curve is estimated, selecting a neighborhood around this point and finding the line of best least-squares fit to the curve in this neighborhood. The mid point $m$ between $P_1$ and $P_2$ is calculated, and connected with the intersection point $t$ between the tangents of these points (see Figure 2(a)). The possible center of the ellipse will lie in the line defined by $\overrightarrow{tm}$. The process is repeated with the points $P_2$ and $P_3$, which define a second line. The intersection of these two lines will be the center of the ellipse.

With the center $c$ of the detected ellipse (see Figure 2(b)) whose coordinates are $(x_c, y_c)$, and the three points $P_1 = (x_1, y_1)$, $P_2 = (x_2, y_2)$, and $P_3 = (x_3, y_3)$ a possible ellipse is estimated as:

- The ellipse equation (derived from Eq. (6)) is defined as:

$$a(x - x_c)^2 + 2b(x - x_c)(y - y_c) + c(y - y_c)^2 = 1 \quad (7)$$

  With the restriction $(ac - b^2) > 0$
- Translating the center to the origin, equation (7) is reduced to:

$$ax^2 + 2bxy + cy^2 = 1 \quad (8)$$

- If the coordinates from $P_1$, $P_2$, and $P_3$ are substituted in equation (8), the following equation system is derived:

$$\begin{bmatrix} x_1^2 & 2x_1y_1 & y_1^2 \\ x_2^2 & 2x_2y_2 & y_2^2 \\ x_3^2 & 2x_3y_3 & y_3^2 \end{bmatrix} \begin{bmatrix} a \\ b \\ c \end{bmatrix} = \begin{bmatrix} 1 \\ 1 \\ 1 \end{bmatrix} \quad (9)$$

- After solving the equation system from (9) the parameters $(x_c, y_c, a, b, c)$ can be estimated.
- The parameter $(x_c, y_c, a, b, c)$ must be converted into polar coordinates $(x_c, y_c, r_1, r_2, \theta)$, where $r_1$ and $r_2$ are the radii of the major and minor axis respectively of the ellipse, and $\theta$ is the angle of rotation for the major axis. In this way the parameter of the ellipse are calculated.

Each found ellipse must be validated [Mac98]. This process is done by drawing the ellipse into the image and looking for all the possible points that exist in the data image and are part of the border of this ellipse. For each valid detected ellipse, a 5-D accumulator is used to aggregate the number of valid ellipses found. Each dimension in the accumulator represents one parameter of the ellipse. After a predefined number of iterations, the cell with the maximum value in the 5-D accumulator determines the parameters for the best ellipse found in the image.

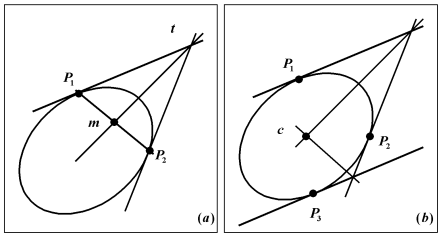


**Figure 2:** *Ellipse Approximation. (a) Estimation of line where the ellipse center should pass. (b) Estimation of the ellipse center.*

## 3. Evaluation

Three different synthetic data sets have been used to evaluate the accuracy of each method described in section 2. Each synthetic data set consists of 3D data of 256x256x768 voxels of $0.5^3$mm, and it simulates a vessel structure of the peripheral arterial tree, from aorta-to-pedal. The diameter of the vessel varies along the z-axis from about 0.7 to about 23 voxels, from the slice 767 to the slice 0. The density for a vessel is defined between 1130 and 1350 and the background density between 1080 and 1100. The curvature of the vessel is simulated by a helix with an angle of 32.14 and radius 76.8. Each data set includes Gaussian noise, which has been added with a $\sigma$ of 0, 5 and 10 respectively. An example of the synthetic data is shown in figure 3. For the evaluation of the centerline estimation several graphs have been generated, describing the error as the distance between the center in the synthetic data, which is known, and the center estimated by the respective method. The RCT, RCMG, EF and RHT methods estimate the vessel centerline and its diameter in individual slices. The CoG and BM estimate just the vessel centerline. Therefore, two types of graphs were generated. The first shows the distance error and the second shows graphically the difference between the real and the estimated diameter of the vessel. Both graphs are plotted along the vessel. Table 1 describes concisely the result of several experiments carried out for each method.

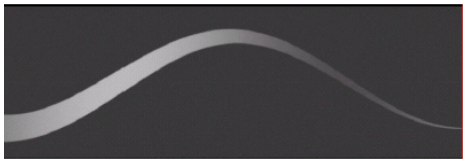

**Figure 3:** *Maximum Intensity Projection of the synthetic data.*

| Method | Mean error (mm) | Comments |
|---|---|---|
| RCT | $\approx 1.11 \pm 0.4$ | - Good approximation along different diameters<br>- Overestimates the diameter<br>- Threshold dependent |
| RCMG | $\approx 1.82 \pm 0.9$ | - Good approximation along different diameters<br>- Overestimates the diameter<br>- Threshold dependent |
| BM | $\approx 0.99 \pm 0.63$ for vessel diameter <5mm | - Time consuming<br>- Requires an optimization process<br>- Better for small vessel (<5mm of diameter) than large vessel |
| CoG | $\approx 0.8 \pm 0.4$ | - Best center approximation along different diameters |
| EF | $\approx 0.56 \pm 0.22$ | - Edge detector dependent<br>- Not robust enough |
| RHT | $\approx 5.23 \pm 6.89$ | - Fails many times especially for small vessel<br>- In general there are not enough points in a vessel cross-section available to get significant results<br>- Not robust enough<br>- Computationally expensive |

**Table 1:** *Comparison of the evaluated methods.*

The RCT, RCMG and CoG use threshold values to consider vessel pixels. These values were determined empirically based on the density distribution analysis of vessels on CTA data done by Kanitsar et al. [KPF*01]. For the evaluation these values were varied accord with the data set. The selection of a good threshold interval to identify vessel pixels results in a better approximation of the center. Figures 4(a, b and c) show the distance error gotten with these methods. These graphs show how CoG exhibits better results than RCT and RCMG. The BM requires an optimization process. The figure 4(d) show how this method gets worst results on large (slice 0 to $\approx$ 500) than on small vessels.

The EF and RHT use the Canny edge detector. This detector uses two threshold values for the "hysteresis process" involved in the method, which classify the pixels resulting from previous Gaussian filtering, gradient and non-maximum suppression steps [Can86]. The threshold values used for the Canny edge detector were modified, but were not able to achieve better results for small vessels. Peaks in figures 4(e,f) show where the methods fail because of the Canny edge detector or there are not enough points to extract the parameters of the ellipse using EF or RHT techniques. The method from MacLaughlin [Mac98] was used to implement the RHT. Many parameters and threshold values must be handle in a precise way. This makes an accurate evaluation of this method for small diameter difficult. In general, RCT, RCMG, EF and RHT overestimate the diameter approximation of the vessels (see figure 5).

Timing are giving in table 2. While BM and RHT clearly have the longest execution times, RCT, RCMG, and CoG are very fast and do no exhibit significant performance differences. EF is slower than the latter three methods, but still tolerable.

### 3.1. Improvements

The RCT, RCMG and CoG can be improved using an adaptive threshold estimation during the centerline process. The BM require to optimize the search process for the best matching, and could be implemented using sub-pixel precision for a best approximation. For EF and RHT is important

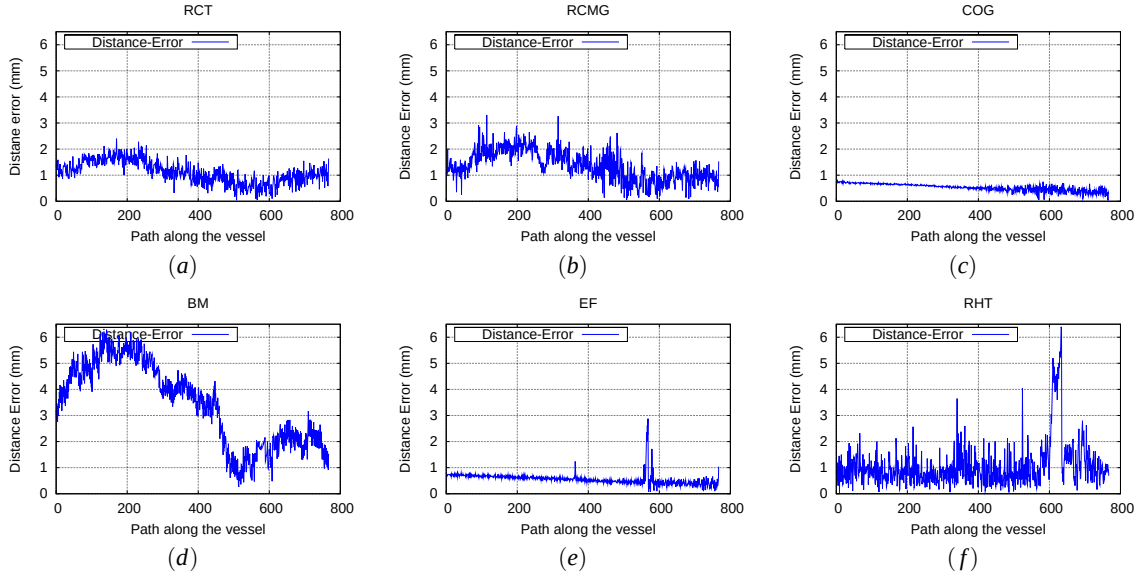


**Figure 4:** *Distance error graphs of the center estimated by (a) RCT, (b) RCMG, (c) CoG, (d) BM, (e) EF, and (f) RHT method*

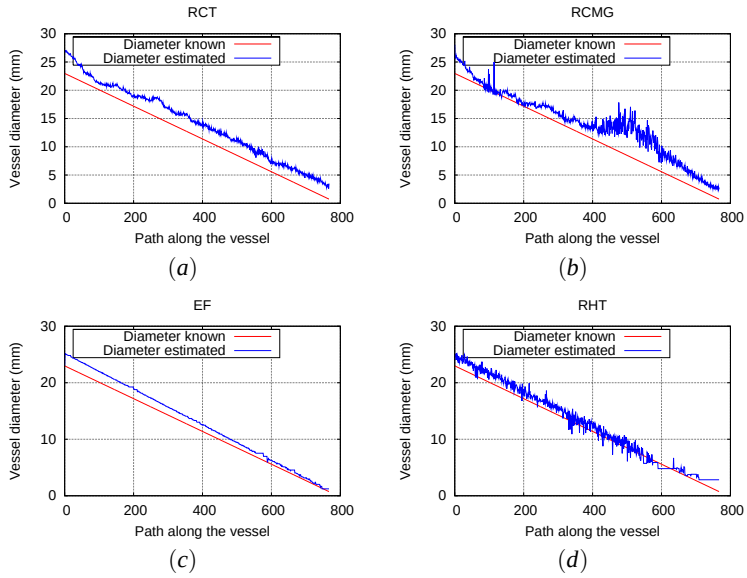


**Figure 5:** *Diameter estimated by (a) RCT, (b) RCMG, (c) EF, and (d) RHT method*

to use a very good edge detector or refine the threshold values used by the Canny edge detector. The RHT technique that have been used in this work requires a refining process of all parameters involved in the method.

## 4. Conclusion

The paper presents an evaluation of different techniques to approximate the center of the vessel in the peripheral arterial tree. Synthetic data sets were used in order to evaluate the accuracy of each method. In general all methods are sensitive to noise. The CoG method exhibits less sensitivity to noise

| RCT | RCMG | EF | CoG | BM | RHT |
|---|---|---|---|---|---|
| 1.797 | 1.594 | 3.969 | 1.531 | 174,000 | 104,000 |

**Table 2:** *Execution times in seconds for each evaluated method.*

than the other techniques. The RCT, RCMG and CoG methods provide the best approximation to the center. The BM technique requires an optimization process for better results. The EF technique depends on the parameters of the Canny edge detector. The RHT technique also depends on the parameters of the Canny edge detector, and is computationally expensive.

The methods analyzed were selected as result of an exploration of different methods used to determine elliptical shapes and detect the object's center. In this study, the RCT method is the only one used for centerline detection of vessel structure. The other methods are not already used in this area, but they were considered because simplicity, novelty in the area, few sensitivity to noise and attack the problem.

The centerline estimation of the peripheral arteries is a difficult task, because of the partial volume effect, diameter of small vessels (tibial and fibular arteries), overlapping of density values between vessels, bones and soft tissues. Therefore, this topic continues being an open problem. The results presented in this work are encouraging us to further develops in these algorithms.

## References


[BFC03] BÜHLER K., FELLED P., CRUZ A. L.: Geometric methods for vessel visualization and quantification - a survey. In *Geometric Modelling for Scientific Visualization* (2003), G. Brunnet, B. Hamann and H. Müller and L. Linsen (eds.). Kluwer Academic Publishers, pp. 399–420. 1

[Can86] CANNY J.: A computational approach to edge detection. *IEEE Trans. Pattern Anal. Machine Intell. 8*, 6 (1986), 679–698. 3, 4

[CRC92] COATRIEUX J. L., RONG J., COLLAREC R.: A framework for automatic analysis of the dynamic behavior of coronary angiograms. *Inter. J. Cardiac Imag. 8* (1992), 1–10. 1

[DKF95] DAVIS C. Q., KARU Z. Z., FREEMAN D. M.: Equivalence of subpixel motion estimators based on optical flow and block matching. In *Inter. Symp. Computer Vision* (1995), pp. 7–12. 2

[FF95] FITZGIBBON A., FISHER R.: A buyer's guide to conic fitting. In *British Machine Vision Conference* (1995), pp. 513–522. 3

[KPF*01] KANITSAR A., PREGENITAL R., FELLED P., FLEISCHMANN D., SANDNER D., GRÖLLER E.: Computed tomography angiography: a case study of peripheral vessel investigation. In *IEEE Visualization* (Oct 2001), pp. 477–480. 1, 2, 4

[KQ00] KIRBAS C., QUEK F.: *A Review of Vessel Extraction Techniques and Algorithms*. Tech. rep., VisLab Wright State University, Dayton, Ohio, Nov 2000. 1

[Mac98] MACLAUGHLIN R. A.: Randomized Hough Transform: Improved ellipse detection with comparison. In *Pattern Recognition Letters 19* (1998), pp. 299–305. 3, 4

[NKSK93] NIKI N., KAWATA Y., SATO H., KUMAZAKI T.: 3D imaging of blood vessels using x-ray rotational angiographic system. In *Medical Imaging Conference* (1993), IEEE, pp. 1873–1877. 1

[PGJ03] PAREDOS P., GOLOB M., JENSTERLE M.: Interrelationship between peripheral arterial occlusive disease, carotid atherosclerosis and flow mediated dilation of the brachial artery. *Inter. Angiology* (Mar 2003). 22(1):83-7. 1

[Pui98] PUIG A.: *Cerebral Blood Vessels Modelling*. Tech. Rep. LSI-98-21-R, Universitat Politècnica de Catalunya, 1998. 1

[TKN*95] TOZAKI T., KAWATA Y., NIKI N., OHMATSU H., MORIYAMA N.: An approach for detecting blood vessel diseases from cone-beam ct image. In *IEEE Nuclear Science Symposium and Medical Imaging Conference* (1995), pp. 1470–1474. 1

[vAEPR02] VAN ASSEN H., EGMONT-PETERSEN M., REIBER J.: Accurate object localization in gray level images using the center of gravity measure; accuracy versus precision. *IEEE Trans. Imag. Proc. 11*, 12 (Dec 2002), 1379–1384. 2

[WNV00] WINK O., NIESSEN W., VIERGEVER M.: Fast delineation and visualization in 3D angiographic images. *IEEE Trans. Med. Imag. 19*, 4 (2000), 337–346. 1, 2

[XOK90] XU L., OJA E., KULTANEN P.: A new curve detection method: Randomized Hough Transform (RHT). In *Pattern Recognition Letters* (1990), pp. 331–338. 3

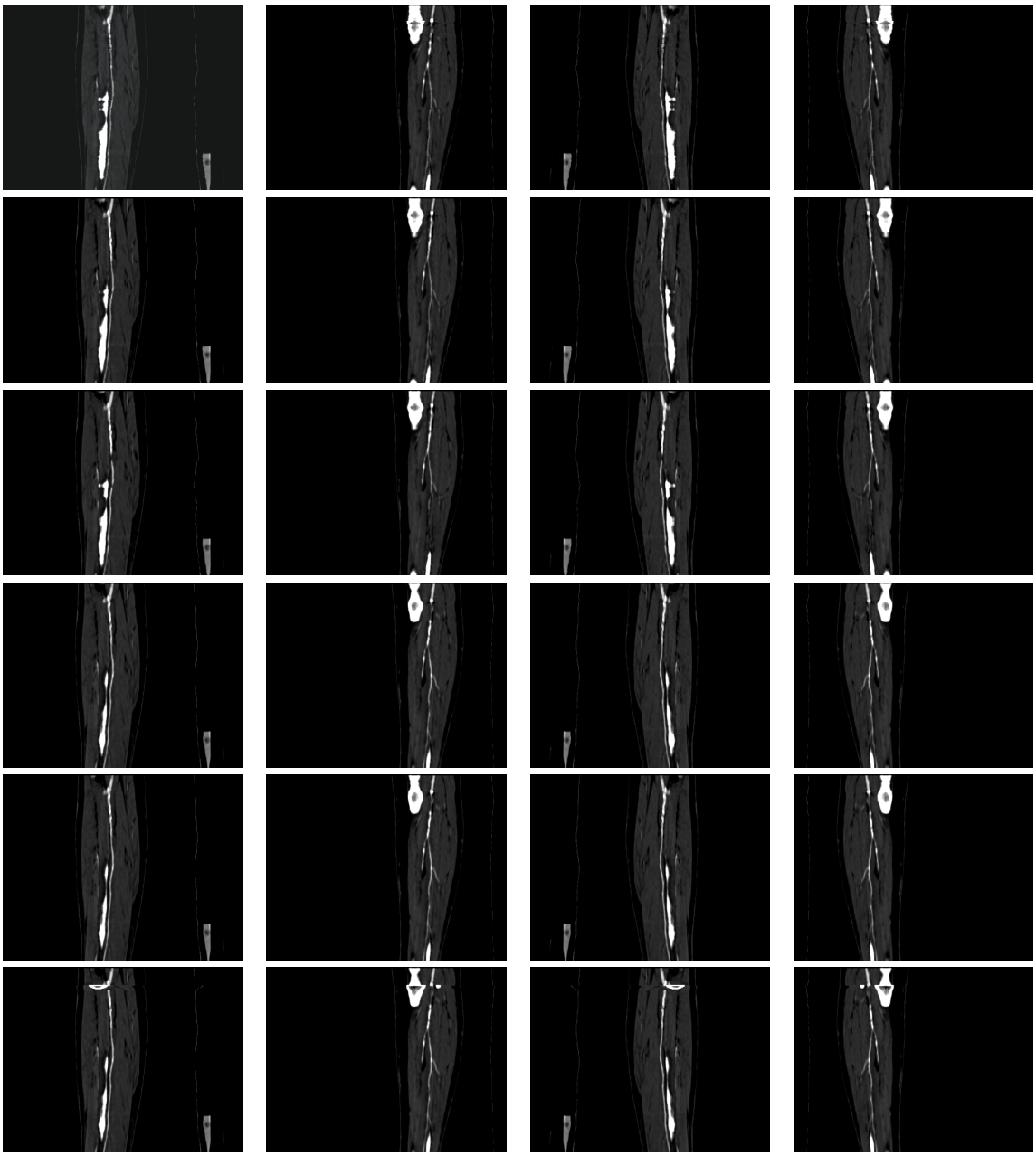

**Figure 6:** *From left to right rotating CPR with 45, 135, 225 and 315 degree. From top to bottom centered with RCT, RCMG, CoG, EF, BM and RHT. This data corresponds to a femoral with a diameter between 2mm and 4mm, and present a calcification part and one bifurcation. Brighter objects correspond to bone structures. Observing, from left to right, from top to button, the third image exhibits the best approximation center in different rotations of the CPR. This is without consider bifurcations, and corresponds with the CoG method. In this data the best result is exhibited by the RCMG method.*